DOI 10.1007/s10946-024-10186-6
Journal of Russian Laser Research, Volume 45, Number 1, January, 2024

LASER-INDUCED HYPER-SOUND SURFACE ACOUSTIC WAVES AS A PROBE OF EXTENDED DEFECTS IN CRYSTALLINE CdZnTe

N. Yu. Frolov* **and A. I. Sharkov**

Lebedev Physical Institute, Russian Academy of Sciences
Leninskii Prospect 53, Moscow 119991, Russia
*Corresponding author e-mail: n.frolov @ lebedev.ru

Abstract

For CdZnTe crystals containing extended defects – coherent and incoherent twin boundaries, as well as lamellar systems of twins, we measure the propagation patterns of surface acoustic waves (SAW) in the gigahertz range excited by a sharply focused femtosecond laser pulse. Comparison of the calculated SAW radial velocities with experimental data allows us to determine the local crystallographic orientation of crystal regions with defects. We discover strong anisotropic scattering of SAW at twin boundaries and show that the structure of the twin boundary can be determined from the pattern of SAW scattering. Also, we demonstrate the non-reciprocal SAW propagation in lamellar twin systems, as well as quasi-waveguide SAW propagation along the lamellar twin layer.

Keywords: laser ultrasound, surface acoustic waves, twinning system, nondestructive evaluation.

1. Introduction

Extended defects in Group II-VI semiconductors and heterostructures based on them are characterized by considerable local disorder, leading to a significant modification of the electronic subsystem [1–3]. Therefore, it is necessary to develop methods that allows one to simultaneously study both distortions of the crystal structure and modification of the electronic subsystem caused by these distortions.

For the solution of the first problem, the use of non-contact optical methods, that allow determining crystallographic orientation and monitoring its local disturbances by analyzing the propagation pattern of surface acoustic waves (SAW), may be promising [4]. Together with conventional optical microscopy and spectroscopy, these methods enable combined studies of the crystal structure, electron spectrum, and dynamic processes in the electron subsystem with a spatial resolution of about 1 μm. A previous study of SAW propagating along low-symmetry surfaces of CdZnTe single crystals [5] showed that the problem of determining the local crystallographic orientation can be solved with reasonable accuracy.

The main goal of this work is to investigate the SAW scattering by the boundaries of coherent and noncoherent twins, and also twinning systems emerging at the crystal surfaces, using the methods of picosecond acoustics (pump-probe).

2. Samples and Experimental Setup

We perform our experiments on $Cd_{0.95}Zn_{0.05}Te$ plates cut from a bulk crystal, grown by vertical directed crystallization, using the Bridgman method. The crystallographic orientation of the samples

Manuscript submitted by the authors in English on December 12, 2023.

is verified using X-ray diffraction analysis. Crystals are selected that simultaneously contain regions with the $(1\,1\,1)$ and $(\bar{1}\,\bar{1}\,\bar{5})$ orientations, with boundaries that can be coherent, meaning that the bonds between the boundary atoms of adjacent regions are similar to the bonds in a perfect crystal. In Fig. 1 a, we show a diagram of a twin with a coherent boundary. When twinning occurs in the $(\bar{1}\,\bar{1}\,1)$ plane, i.e., rotating 180° around the $[\bar{1}\,\bar{1}\,1]$ axis, the bonds in the crystal do not change, but the cut surface $(1\,1\,1)$ turns into $(\bar{1}\,\bar{1}\,\bar{5})$. The crystals under study contain both coherent and incoherent boundaries. The lines of intersection of the coherent and incoherent twinning planes with the crystal surface intersect at an angle of 120°.

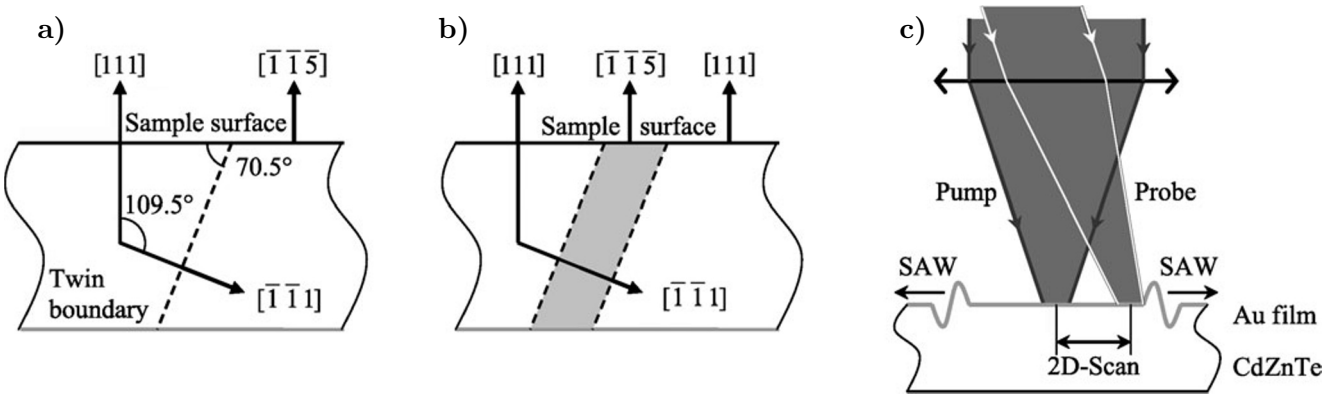

Fig. 1. Crystallographic diagram of a coherent twin boundary in the samples under study (a), crystallographic diagram of a lamellar layer (b), and experimental schematic (c).

On the surface of the crystals under study, we also discover the regions with so-called "lamellar" twin systems. These systems consist of the crystal layer sandwiched between two parallel twinning planes. In the case of coherent boundaries, this means the appearance of a thin layer with an orientation different from the main orientation of the crystal. This occurs due to the fact that, at the first coherent boundary, the crystal rotates 180°, and at the second boundary, it rotates another 180°, i.e., coincides with itself. The diagram of such a twin is shown in Fig. 1 b.

To enhance the efficiency of SAW optical excitation, a 50 nm thick Au film is thermally deposited on the surface of each plate. The thickness of the Au film is chosen to be small to exclude SAW dispersion up to frequencies of ∼2 GHz.

In Fig. 1 c, we show the geometry of the experiment. A femtosecond excitation pulse of the second harmonic of a Titanium-sapphire laser is focused on a 1.5 μm diameter spot at the surface of the sample (pump). The parameters of the pulse are as follows: $\tau = 160$ fs, $\lambda = 400$ nm, and $E = 0.4$ nJ. The minor $(10^{-6} - 10^{-3})$ changes in amplitude and phase of the first-harmonic pulse (the probe pulse) of the same laser beam ($\lambda = 800$ nm), reflected by a sample surface, are detected with a Sagnac interferometer [6].

To measure the dynamics of the reflection coefficient, we use an optical delay line, which made it possible to change the delay between the pumping and probing pulses. The sequence of exciting pulses is modulated, using a Pockels cell to implement the synchronous detection technique. The optical scheme is similar to that shown in [7], except that we install the 4F scanner in the probing channel. To study spatial and temporal distribution of the wave field, the surface of the specimen is scanned with the probe beam. The sensitivity reaches ∼1 μrad for the phase and $\sim 10^{-6}$ for the amplitude of the reflection coefficient, respectively, the spatial resolution is ∼1.5 μm, and the time resolution is <1 ps.

3. Experimental Results and Discussion

In Fig. 2 a, b, we show the calculated angular dependence of the radial velocity of the Rayleigh mode for the (1 1 1) cut and for the $(\bar{1}\,\bar{1}\,\bar{5})$ cut, respectively. Calculations are carried out similarly to [8] in the model of a semi-infinite medium described by an anisotropic elasticity tensor [9]. It was shown in [5] that the region orientations can be determined by the shape of the SAW wavefronts. Rayleigh waves can be most reliably identified.

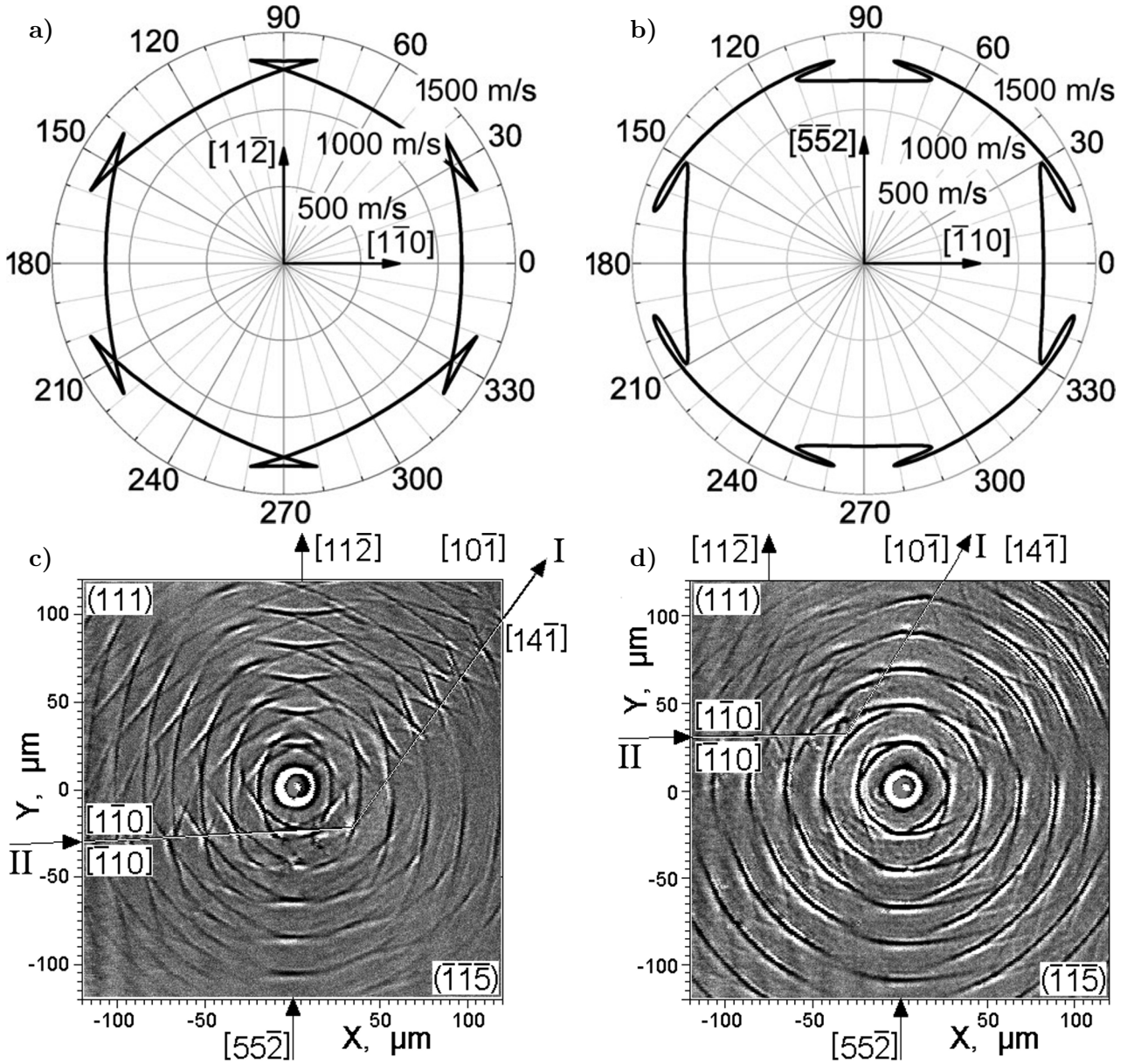

Fig. 2. Angular dependence of the SAW ray velocity calculated for the (1 1 1) crystal cut (a) and the $(\bar{1}\,\bar{1}\,\bar{5})$ crystal cut (b). Experimental SAW propagation patterns in CdZnTe near twin boundaries with the excitation point located in the (1 1 1) crystal cut (c) and the $(\bar{1}\,\bar{1}\,\bar{5})$ crystal cut (d).

In Fig. 2 c, d, we show SAW propagation patterns near the twinning boundaries. These patterns consist of a set of concentric contours corresponding to propagating surface waves excited by successive pump pulses repeated every 13.2 ns. In Fig. 2 c, the shape of the wavefronts indicates that the region near the excitation point has the (1 1 1) orientation. Discontinuities in the SAW fronts indicate the presence of boundaries, marked by black lines I and II. One can see that the boundaries intersect at an angle of 120°, and both boundaries are perpendicular to the directions equivalent to $[1\,1\,\bar{2}]$. The wavefront shapes significantly differ on different sides of the boundary, which is associated with differences in crystallographic orientation. A change in the crystallographic orientation, when passing through the boundary, leads to a corresponding change in the elasticity tensor, resulting in discontinuities and

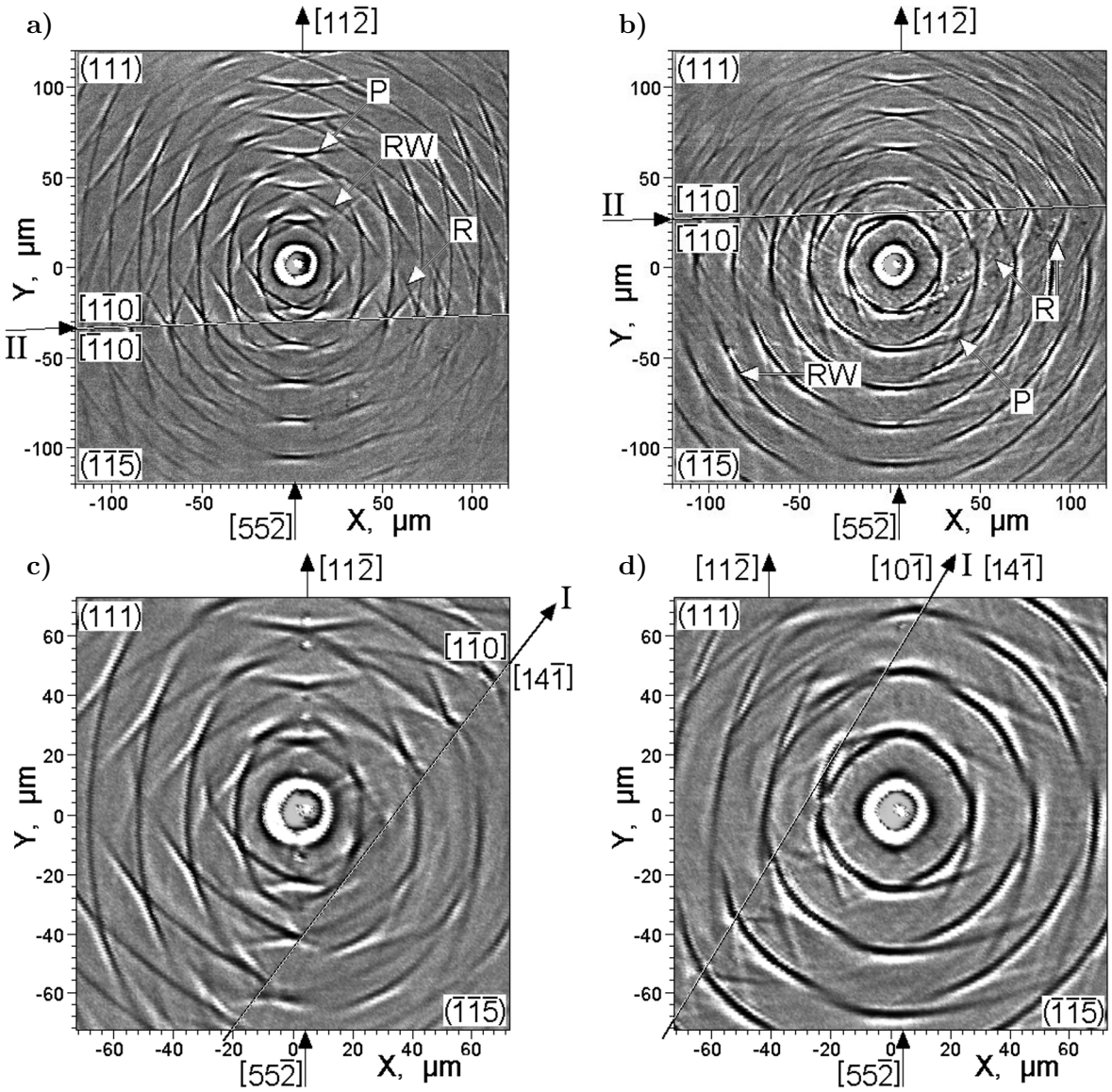

Fig. 3. Experimental SAW propagation patterns in CdZnTe near a coherent twin boundary with the excitation point located in the (1 1 1) crystal cut (a) and in the $(\bar{1}\,\bar{1}\,\bar{5})$ crystal cut (b). A noncoherent twin boundary with excitation point located in the (1 1 1) crystal cut (c) and in the $(\bar{1}\,\bar{1}\,\bar{5})$ crystal cut (d).

distortions of the fronts, as well as reflections from the boundary. In Fig. 2 d, the shape of the wave fronts shows that the region near the excitation point has the $(\bar{1}\,\bar{1}\,\bar{5})$ orientation.

The features and discontinuities on the wave fronts allows for the identification of the type of twinning boundaries. The boundary line II in Fig. 2 c, d is perpendicular to the $[1\,1\,\bar{2}]$ direction in the region with the $(1\,1\,1)$ orientation and the $[\bar{5}\,\bar{5}\,2]$ direction in the region with the $(\bar{1}\,\bar{1}\,\bar{5})$ orientation. So this boundary lies in the $(\bar{1}\,\bar{1}\,1)$ plane; see Fig. 1 a; therefore, it is coherent.

The location of the SAW fronts relative to the boundaries is shown in more detail in Fig. 3. In Fig. 3 a, c, excitation occurs at the $(1\,1\,1)$ cut, and the wavefront pattern has the 6th order symmetry. In Fig. 3 b, d, excitation occurs at the $(\bar{1}\,\bar{1}\,\bar{5})$ cut, and the wavefront pattern has the 2nd order symmetry. In Fig. 3 a, b, the wavefronts of the Rayleigh wave, pseudo-surface wave, and reflection from the twinning boundary are shown with the help of arrows labeled by RW, P, and R, respectively.

When crossing the boundary, the symmetry of the SAW pattern decreases. Here, we can also observe discontinuities of SAW fronts at the boundary. One can see that the SAW amplitude more strongly decreases, when moving from the $(1\,1\,1)$ region to the $(\bar{1}\,\bar{1}\,\bar{5})$ region than in the opposite direction.

In Fig. 3 c, d, the wave fronts recorded near the boundary located at an angle of 120° to the coherent boundary are shown. It is clear from the wavefront patterns, that this boundary corresponds to the symmetry of the sample region with the $(1\,1\,1)$ orientation, but does not correspond to the symmetry of the region with the $(\bar{1}\,\bar{1}\,\bar{5})$ orientation. Therefore, this boundary I corresponds to an incoherent twinning plane.

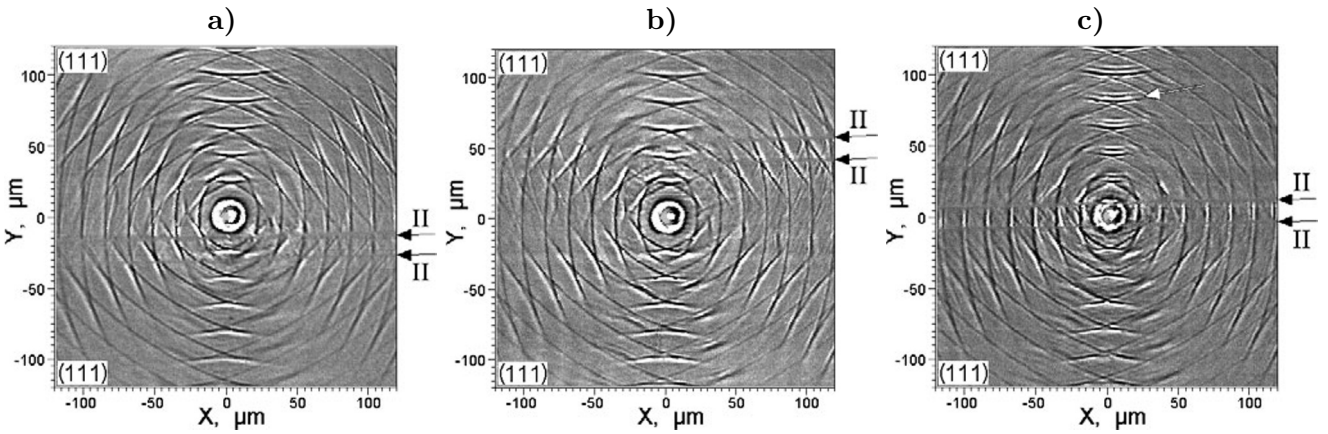

Fig. 4. SAW field patterns during the laser excitation on one side (a) and the other side (b) of the lamellar layer, and during the laser excitation in the middle of this layer (c).

In Fig. 4 a, b, we show the SAW field patterns during the laser excitation on one and the other side of the lamellar layer with the $(\bar{1}\,\bar{1}\,\bar{5})$ orientation and a thickness of ∼20 μm, marked by two black arrows, and in Fig. 4 c, we show the SAW field pattern during the laser excitation in the middle of this layer.

When generated outside the layer, the SAW patterns, with the exception of features near the excitation region, are similar. However, when the laser spot is in the middle of the layer, the SAW patterns above and below the layer are different. Thus, in a ray propagating perpendicular to the boundaries of the layer (i.e., in the $[1\,1\,\bar{2}]$ direction), corresponding to a pseudo-surface wave above the layer, the front breaks up into three parts propagating one after the other (marked by white arrow). This phenomenon is not observed in the wave below the layer. This asymmetry can be caused by an inclination of the twinning planes relative to the sample surface by 70.5°; see Fig. 1 a, b.

One can see that a localized wave propagates between the twin planes along the surface of the layer (marked by white arrow). The speed of this wave is 1.28 μm/ns, which is close to the speed of the Rayleigh wave. However, its intensity is higher than the intensity of the Rayleigh wave in neighboring regions, which allows us to consider it as propagating in a quasi-waveguide mode.

4. Summary

Thus, as a result of optical excitation and detection of SAW on the CdZnTe crystal surface, one can determine the local crystallographic orientation of the sample. The strong anisotropy of SAW scattering on extended defects (twinning boundaries) allows for their visualization and structural determination. In particular, the technique used enables differentiation between coherent and incoherent twinning planes. We observed a quasi-waveguide SAW propagation in a lamellar twin. To further develop the technique and reliable interpretation of experimental data, it is necessary to simulate the SAW scattering on extended defects, which is a difficult task due to elastic anisotropy as well as the SAW conversion into bulk modes.

Acknowledgments

This study was supported by the Russian Science Foundation under Grant No. 19-79-30086. Authors are grateful to Dr. A. Yu. Klokov for valuable discussions.

References

1. K. E. Kweon, D. Aberg, and V. Lordi, *Phys. Rev. B*, **93**, 174109 (2016); DOI: 10.1103/PhysRevB.93.174109
2. C. Li, Y. Wu, T. J. Pennycook, et al., *Phys. Rev. Lett.*, **111**, 096403 (2013); DOI: 10.1103/PhysRevLett.111.096403
3. V. Babentsov, V. Boiko, G. A. Schepelskii, et al., *J. Lumin.*, **130**, 1425 (2010); DOI: 10.1016/j.jlumin.2010.03.006
4. D. H. Hurley, O. B. Wright, O. Matsuda, et al., *Phys. Rev. B*, **73**, 125403 (2006).
5. A. Yu. Klokov, V. S. Krivobok, A. I. Sharkov, et al., *JETP Lett.*, **106**, 503 (2017); DOI: 10.1134/S0021364017200097
6. T. Tachizaki, T. Muroya, O. Matsuda, et al., *Rev. Sci. Instrum.*, **77**, 043713 (2006).
7. A. Yu. Klokov, A. I. Sharkov, V. G. Ralchenko, et al., *J. Russ. Laser Res.*, **77**, 580 (2021); DOI: 10.1007/s10946-021-09996-9
8. G. W. Farnell, *Physical Acoustics*, **6**, 109 (1970).
9. H. J. McSkimin and D. G. Thomas, *J. Appl. Phys.*, **33**, 56 (1962).